ASEAN Engineering Journal

Full Paper

VOLTAGE STABILITY ASSESSMENT OF LARGE-SCALE PHOTOVOLTAIC SYSTEMS USING SIMULATION-BASED MODELLING AND VCPI ANALYSIS

Nurfaraliyana Samburi[a]*, Ahmad Fateh Mohamad Nor[a], Suriana Salimin[a], Nur Ellysa Mu'izz Mohd Zaini[b]

[a]Green and Sustainable Energy Focus Group, Faculty of Electrical and Electronic Engineering, Universiti Tun Hussein Onn Malaysia (UTHM), 86400 Parit Raja, Batu Pahat, Johor, Malaysia

[b]Favelle Favco Cranes (M) Sdn. Bhd. Negeri Sembilan, 42 Persiaran Bunga Tanjung 2, Senawang Industrial Park, 70400 Seremban, Negeri Sembilan, Malaysia

Article history
Received
27 March 2025
Received in revised form
02 December 2025
Accepted
21 January 2026
Published online
31 August 2026

*Corresponding author
afateh@uthm.edu.my

Graphical abstract

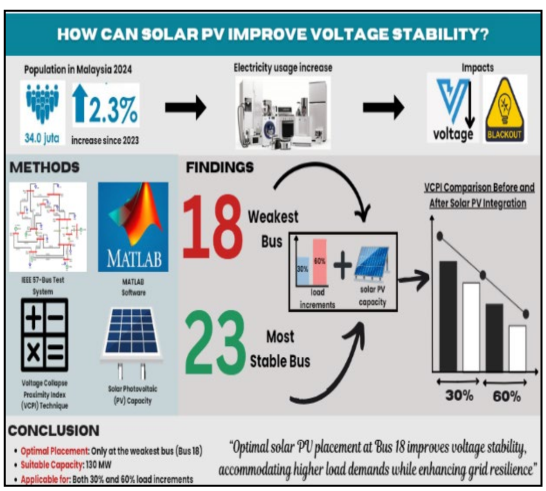

Abstract

The increasing electricity demand presents significant challenges for the power system in maintaining stable and reliable operation. These challenges place stress on electrical power grids, particularly the distribution system, and may lead to power disruptions and blackouts if not managed effectively. This research focuses on analyzing voltage stability to ensure that voltage levels remain within the acceptable range of 0.95 pu to 1.05 pu under both normal and increased loading conditions. As electricity demand increases, voltage instability can occur and requires effective assessment methods to identify buses that are prone to instability, since initial voltage values are not enough to determine stability. The methodology is proposed using MATLAB software to assess the voltage stability of the IEEE 57-bus test system. The Voltage Collapse Proximity Index (VCPI) is used as an effective indicator to identify the weakest and the most stable buses in the network. The analysis shows that Bus 18 is the weakest bus and Bus 23 is the most stable bus. Next, solar PV is integrated into both buses, and the system is tested under load increment conditions of 30% and 60%. The results reveal that the optimal placement for solar PV is only at the weakest bus, Bus 18, with a suitable capacity of 130 MW for both load increments. Additionally, the VCPI values decrease after installing solar PV, demonstrating that solar PV can support the higher load demand while enhancing grid resilience and reducing the risk of voltage instability.

Keywords: Voltage Stability, IEEE 57-Bus Test System, VCPI, Solar PV Integration, Load Increments

1.0 INTRODUCTION

Electricity plays a vital role in sustaining daily activities across residential, commercial, and industrial sectors. It is utilized for household lighting, powering appliances, enabling communication networks, and supporting industrial operations. As a result, the demand for electricity continues to rise, driven by population growth, industrial expansion, and the widespread adoption of modern technologies. Studies indicate that total energy consumption currently stands at 20% and is expected to increase by 50% in 2050 [1]. Besides that, electricity demand is directly linked to the electrical power grids, which are networks that generate, transmit, and distribute electricity to consumers. When electricity demand exceeds normal levels, the distribution system carries heavier loads, putting significant stress on the entire electrical power grid [2]. If not managed effectively, this overload can lead to power disruptions and blackouts in the distribution system [3, 4]. Therefore, this research aims to ensure the stability and reliability of electricity networks even when handling higher electricity demand from consumers.

In the context of power systems, voltage stability is a crucial parameter that must be maintained. It is defined as the capability of the power system to maintain stable voltage levels at all buses under normal operating conditions and after being subjected to disturbances [5, 6]. This indicates that under normal operating conditions, the voltage remains stable within acceptable ranges. However, when disturbances occur in the system, the voltage becomes unstable which can result in uncontrollable decline in voltage levels. Fasina et al. (2021) state that the voltage magnitudes at each bus must comply with the IEEE standard range of 0.95 pu to 1.05 pu with ±5% to be considered stable [7, 8]. Therefore, this research proposes to study electricity flows and their impacts on voltage stability using the IEEE 57-bus system as a test model. For instance, Morked and Wang (2024) evaluated voltage stability on three bus systems, IEEE-30, IEEE-57, and IEEE-118 buses [9]. This demonstrates that the IEEE-57 bus remains suitable and widely accepted for assessing voltage stability studies under various loading conditions. In the present study, the analysis focuses on a single bus of the medium-sized IEEE-57 bus system which serves as a connection point to facilitate electricity flow within the electrical power grid, where multiple generators and loads are interconnected. Studying this bus system allows researchers to identify critical buses prone to voltage instability and develop strategies to enhance overall grid performance.

Furthermore, one of the challenges to consider is that identifying critical buses leading to voltage instability is not as simple as examining initial values such as voltage magnitudes. This approach may be insufficient for accurately assessing stability, especially as electricity demand continues to rise under various scenarios. As a solution to arising challenges, the Voltage Collapse Proximity Index (VCPI) is highlighted as an effective indicator for evaluating the voltage stability of all buses in a complex power system [10]. VCPI is also one of the simplest and fastest methods for predicting voltage instability [11]. Chaithra et al. (2018) conducted a voltage stability analysis for power flow studies using the IEEE-14 bus system to test the effectiveness of VCPI. The results indicate that Bus 6 is the weakest bus, with the highest VCPI value of 0.02987 among all the buses. In contrast, Bus 9 is identified as the most stable bus, with a value of 0.00397, the smallest compared to other buses, and almost close to zero [12].

Identifying the critical bus does not eliminate challenges in the electrical power grid as increasing electricity demand continues to strain the system. As overall demand rises, further improvements are required such as upgrading the system by installing new transmission lines and substations. However, this approach represents significant limitations due to its high cost and the extensive time required for implementation. To effectively address stability challenges, the integration of solar photovoltaic (PV) as a grid-tied system into the existing electrical power grid has been proposed. This is because solar PV has a greater impact on grid stability compared to other energy sources [13, 14]. It also contributes to the reduction of greenhouse gas emissions while meeting the growing electricity demand [15]. Solar PV may not be installed across the entire bus system due to limited surface area and the complexity of installations. Consequently, the placement of the solar PV system has become a critical consideration, as random installation without careful planning can pose challenges to voltage stability enhancement [16, 17, 18].

It should be noted that regardless of placement, the capacity of the solar PV must be carefully evaluated to ensure it is appropriately sized to meet the expected power demand. In this study, the solar PV capacities considered range from small to large-scale capacities in megawatts. Although the output of large PV systems can be affected by the weather conditions, the scope of this study is limited to steady-state PV output. For instance, if the solar capacity is 100 MW, the analysis assumes exactly 100 MW without accounting for factors that could influence the output. This limitation is applied to focus on evaluating the impacts of solar PV capacity on voltage stability without introducing the additional complexity of weather variations.

To conduct this research study, the VCPI will be used to identify the weakest and most stable buses. This will allow an evaluation of their performance under various load conditions and an assessment of the impact of solar PV systems. Subsequently, the optimal placement and adaptive capacity of the solar PV will be determined based on whether it should be installed at the weakest or the most stable bus. This study addresses a research gap, as previous studies have not evaluated voltage stability in the IEEE 57-bus test system under various load conditions using VCPI.

2.0 METHODOLOGY

2.1 IEEE 57-Bus Test System

Figure 1 presents the single-line diagram of the standard IEEE 57-bus test system. The test system model was developed based on this diagram, as it provides the detailed specifications for buses, generators, transformers, and transmission lines [19]. The IEEE 57-bus test system consists of three types of buses: a slack bus, generator buses, and load buses. In this system, Bus 1 serves as the slack bus, while the system includes seven generator buses, specifically Bus 2, Bus 3, Bus 6, Bus 8, Bus 9, and Bus 12. The remaining 42 buses serve as load buses and are located within the distribution network [20]. The IEEE-57 bus system was adopted in this study because it continues to be widely used in voltage stability research, as demonstrated by previous studies, and its medium size makes it suitable for comprehensive analysis. Therefore, the research focuses on evaluating the voltage stability by concentrating on load buses which are more prone to voltage instability than generator and slack buses.

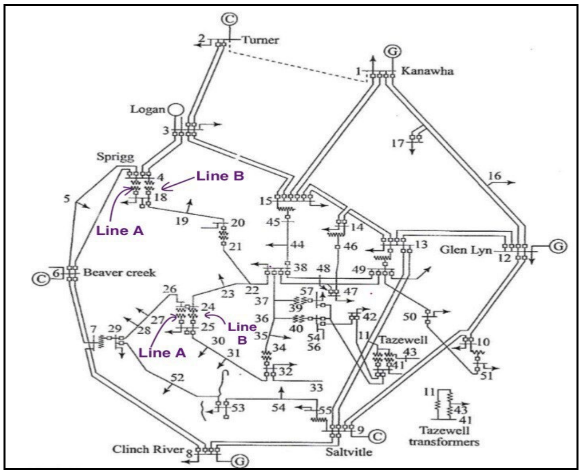

Figure 1 Standard IEEE-57 Bus Test System [20]

The system also includes 17 transformers and 63 transmission lines connected to the buses. Furthermore, as shown in this figure, Bus 18 and Bus 25 are interconnected through two transmission lines, which are referred to as Line A and Line B for ease of reference in the subsequent discussion.

2.2 Power Flow Analysis using the Newton-Raphson Method

In power system analysis, several iterative techniques are available for solving nonlinear algebraic equations such as Gauss-Seidel, Newton-Raphson, and Quasi-Newton. Among these, the Gauss-Seidel and Newton-Raphson methods are the most commonly used for power flow analysis [21]. This research adopts the Newton-Raphson method, as it is widely recognized as one of the most efficient techniques due to its superior accuracy and suitability for large power systems such as the IEEE 57-bus test system [22]. The power flow study is conducted to predict how electricity flows through the power grid under stable operating conditions and to enable the identification of key parameters such as voltage magnitudes.

2.3 Voltage Collapse Proximity Index (VCPI)

The Voltage Collapse Proximity Index (VCPI) is one of the voltage stability indicators used to assess a power system's proximity to instability [16]. This study shows that even when voltage values are within the acceptable range, the VCPI indicates that the system may still be at risk of voltage instability. This indicator has been adopted in this study because it analyzes the stability of each line within the 57-bus system. The VCPI formula can be calculated using Equations (1) and (2) [23].

$$VCPI\ (Power) = \frac{P_r}{P_{r(max)}} \qquad (1)$$

$$VCPI\ (Power) = \frac{Q_r}{Q_{r(max)}} \qquad (2)$$

The numerator represents the real or reactive power transferred to the receiving end, while the denominator signifies the maximum real or reactive power that can be transferred through a line. This can be calculated using Equations (3) to (4) [23], as shown below.

$$P_{r(max)} = \frac{V_s^{\,2}}{Z_s}\frac{\cos\emptyset}{4\cos^2((\theta-\emptyset)/2)} \qquad (3)$$

$$Q_{r(max)} = \frac{V_s^{\,2}}{Z_s}\frac{\sin\emptyset}{4\cos^2((\theta-\emptyset)/2)} \qquad (4)$$

Phase angle in Equation (5) [23],

$$\emptyset = \tan^{-1}\left(\frac{Q_r}{P_r}\right) \qquad (5)$$

Where,

V_s is defined as sending end voltages
Z_s is defined as line impedances
P_r is defined as receiving end real power
Q_r is defined as receiving end reactive power
$\emptyset$ is defined as phase angle
θ is defined as the angle of line impedance

2.4 Simulation-Based Modelling Using MATLAB

MATLAB is a mathematical software, widely used across various industries for its capabilities in matrix operations, algorithm development, and integration with other programming languages [24]. For this study, scripts implementing the Newton-Raphson method were used to perform the power flow analysis [25]. Key parameters, including bus data, line data, impedance values, real and reactive loads, and reactive power limits, were adjusted to align with the standard IEEE 57-bus test system to ensure accurate results. The simulation was then executed, and the voltage magnitude values at each bus were displayed and recorded.

2.5 Maximum Load Capacity for the Weakest and Most Stable Buses

This section analyzes two specific buses which are the weakest bus and the most stable bus, both identified based on the VCPI results. These results serve as the primary reference for further analysis. For instance, Bus 18 is identified as the weakest bus, with a real power of 27.2 MW, a reactive power of 9.8 MVAR, and a voltage magnitude of 0.965 pu. To simulate an increase in electricity demand, the real and reactive power at Bus 18 are incrementally increased by 30% and 60%. For example, a 30% increase in load is calculated by multiplying the original real power of 27.2 MW by 30%, resulting in 8.16 MW, and then adding it to 27.2 MW to obtain a total of 35.36 MW. The same approach is applied to calculate the new reactive power value. This section aims to determine the maximum load demand that both the weakest bus and the most stable bus can support.

The rationale for setting the load increment at 30% and 60% is as follows. Doni Anggara et al. (2025) applied incremental loads of 25% and 50% on an IEEE-33 bus system, using a load step size of 25% [26]. In the present study, the increments are adapted to 30% and 60% on an IEEE-57 bus system, with a load step size of 30%. This is because the larger bus system requires slightly higher steps to observe voltage stability effects. In addition,

these increments represent small and moderate increases in load demand, allowing observation of how voltage stability changes when the system experiences different levels of stress. These also reflect that the power system load is not constant and may increase due to consumer needs.

2.6 Optimal Placement and Suitable Solar PV Capacity for The Weakest and Most Stable Buses

This analysis is a continuation of Section 2.5. The first step is to update the maximum load capacity for both the weakest and the most stable buses in MATLAB. For example, after applying a 30% load increment at the weakest bus, the maximum loads reach 101 MW for real power and 36.39 MVAR for reactive power. Next, solar PV is integrated into the Real Power Generating section of the simulation, as it only provides additional real power to the system. The solar PV capacity is tested across a range of 10 MW to 280 MW to assess its impact on system performance. Based on the analysis results, the optimal placement for solar PV installation whether at the weakest bus or the most stable bus is identified, along with the appropriate solar PV capacity. The selection of suitable solar PV capacity is based on its effectiveness in improving voltage magnitude values within the system.

3.0 RESULTS AND DISCUSSION

3.1 Power Flow Analysis of the IEEE-57 Bus Test System

Table 1 presents the power flow results after inputting all the data for the IEEE-57 bus system and implementing the Newton-Raphson method in MATLAB. The output reveals the voltage magnitudes across the system. The lowest voltage magnitude is recorded at Bus 31, measuring 0.834 pu, with a real load of 5.8 MW and a reactive load of 2.9 MVAR. In contrast, Bus 1 has the highest voltage magnitude at 1.040 pu, with a real load of 55 MW and a reactive load of 17 MVAR.

Table 1 Voltage magnitudes for the IEEE 57-bus test system

Bus Number	Voltage Magnitude (pu)
1	1.040
2	1.000
3	0.975
4	0.963
5	0.950
6	0.950
7	0.940
8	0.955
9	0.950
10	0.945
11	0.942
12	0.965
13	0.945
14	0.941
15	0.968
16	0.977
17	0.999
18	0.965
19	0.961
20	0.971
21	0.960
22	0.966
23	0.963
24	0.940
25	0.883
26	0.902
27	0.929
28	0.946
29	0.961
30	0.862
31	0.834
32	0.852
33	0.850
34	0.915
35	0.923
36	0.933
37	0.943
38	0.972
39	0.941
40	0.931
41	0.960
42	0.929
43	0.975
44	0.980
45	1.009
46	1.025
47	0.995
48	0.988
49	0.996
50	0.981
51	1.008
52	0.925
53	0.912
54	0.949
55	0.994
56	0.929
57	0.924

According to voltage stability standards, the voltage magnitude values at each bus should be maintained within the acceptable range of 0.95 to 1.05 per unit. Several buses, including Bus 7, Bus 10, Bus 11, Bus 13, Bus 14, Bus 24, Bus 26, Bus 27, Bus 28, Bus 34, Bus 35, Bus 36, Bus 37, Bus 39, Bus 40, Bus 42, Bus 52, Bus 53, Bus 54, Bus 56, and Bus 57, show voltage magnitudes below 0.95 per unit. In contrast, Bus 1, Bus 2, Bus 45, and Bus 51 have voltage magnitudes closest to unity (1.0 pu).

3.2 VCPI Analysis for Identifying the Weakest and Most Stable Buses

Table 2 illustrates the VCPI values, which are calculated using the formula from Equations 1 to 5, and all values expressed in per unit. The VCPI analysis was conducted for the load buses, including bus numbers 5, 10, 13, 14, 15, 16, 17, 18, 19, 20, 23, 25, 27, 28, 29, 30, 31, 32, 33, 35, 38, 41, 42, 43, 44, 47, 49, 50, 51, 52, 53, 54, 55, 56, and 57.

Table 2 VCPI values for all load buses

Bus Number	Connected Lines	VCPI (pu)
5	4-5	0.1303
10	9–10	0.0632
13	9–13	0.1914
13	11–13	0.0887
13	12–13	0.0703
14	13–14	0.0382
15	1–15	0.1295
15	3–15	0.0774
15	13–15	0.1271
15	14–15	0.0800
16	1–16	0.5399
16	12–16	0.2133
17	1–17	0.2729
17	12–17	0.4522
18	4–18 (Line A)	1.0359
18	4–18 (Line B)	0.8028
19	18–19	0.1724
20	19–20	0.0850
23	22–23	0.0077
25	24–25 (Line A)	0.6796
25	24–25 (Line B)	0.7071
27	26–27	0.1851
28	27–28	0.0413
29	7–29	0.0690
29	28–29	0.0768
30	25–30	0.0832
31	30–31	0.3505
32	31–32	0.1417
33	32–33	0.0198
35	34–35	0.0467
38	22–38	0.0369
38	37–38	0.1258
41	11–41	0.3554
41	56–41	0.3697
42	41–42	0.2504
42	56–42	0.2531
43	11–43	0.0228
43	41–43	0.0613
44	38–44	0.0471
47	46–47	0.1404
49	13–49	0.2398
49	38–49	0.2650
49	48–49	0.1928
50	49–50	0.23300
51	10–51	0.0775
51	50–51	0.2831
52	29–52	0.0919
53	52–53	0.2117
54	53–54	0.0858
55	9–55	0.0586
55	54–55	0.1388
56	40–56	0.6453
56	57–56	0.1689
57	39–57	0.6550

As presented in Table 2, Bus 18 located on the line between Bus 4 and Bus 18 (Line A), has the highest VCPI value among the load buses at 1.0355 pu. In contrast, the lowest VCPI value is observed at Bus 23 on the line connecting Bus 22 and Bus 23, measuring 0.0077 pu. Additionally, Bus 18 and Bus 25 are connected by two transmission lines designated as Line A and Line B, as shown in the one-line diagram of the 57-bus system.

Based on the VCPI reference, a VCPI value close to zero indicates a stable system, while a value approaching unity (1.0 per unit) is considered critical and signals that the system is nearing instability [27]. As shown in Table 2, Bus 18 is identified as the weakest bus due to its highest VCPI value, which has already reached the critical limit of 1.0 per unit. Bus 18 has a voltage magnitude of 0.965 pu, which is within the acceptable range, but its highest VCPI value indicates that the bus is unstable. In contrast, Bus 23 is identified as the most stable bus, as it has the lowest VCPI value. This highlights the effectiveness of using VCPI in assessing voltage stability. Take Bus 18 and Bus 23 for further analysis.

3.3 Analysis of Maximum Load Capacity for Identified Buses

To determine the maximum load capacity that Bus 18 and Bus 23 can support, the load is increased by 30% and 60% from its initial value. Figure 2 depicts the maximum real power results. The 0% load increment represents the base case or normal operating condition, where Bus 18 records 27.2 MW and Bus 23 records 6.3 MW. When the load increased to 30%, the maximum real power at Bus 18 increases to 101 MW, and Bus 23 reaches 146.9 MW. At a 60% load increment, Bus 18 further increases to 111.41 MW, while Bus 23 reaches 169.41 MW. According to the results, Bus 23 stands out as the most stable bus which is capable of effectively supporting higher real loads at 30% and 60% increments.

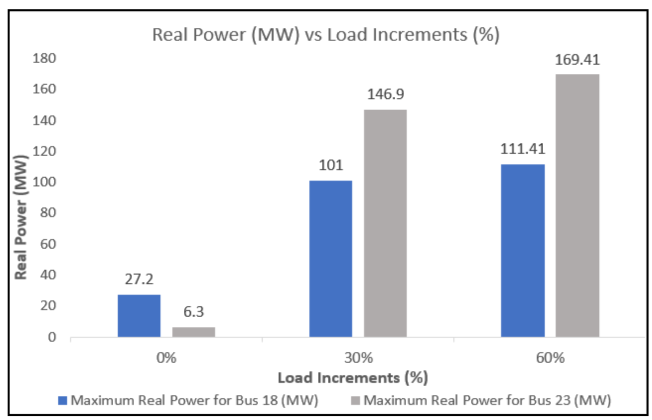

Figure 2 Maximum real power values

Figure 3 shows the maximum reactive power results. At the base case (0% load increment), Bus 18 and Bus 23 record 9.8 MVAR and 2.1 MVAR. With a 30% load increment, Bus 18 achieves 36.39 MVAR, while Bus 23 reaches 48.91 MVAR. At a 60% load increment, Bus 18 reaches 40.14 MVAR, while Bus 23 attains 56.4 MVAR.

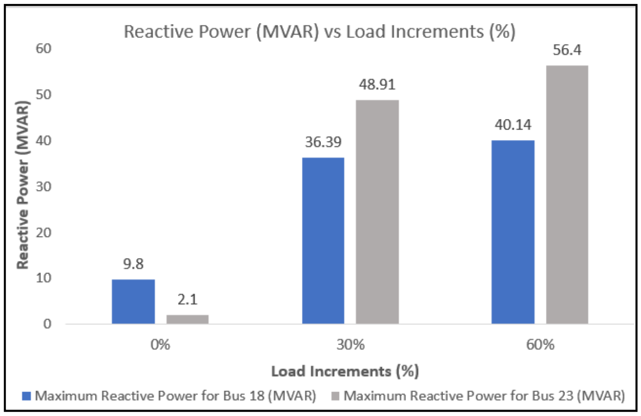

Figure 3 Maximum reactive power values

3.4 Solar PV Integration at the Identified Weakest Bus

At a 30% load increment, the maximum load capacity at Bus 18 reaches 101 MW and 36.39 MVAR. The next step is to test these maximum load values with different solar PV capacities as shown in Table 3. Initially, the voltage magnitude is 0.965 pu, however, as the load increases, it drops to 0.775 pu. Following the installation of the solar PV, the voltage gradually recovered, reaching a maximum of 0.9 pu when the solar PV capacity ranged from 110 MW to 140 MW.

Table 3 Solar PV integration at Bus 18 under 30% load increment

Solar PV Capacity (MW)	Voltage Magnitude (pu)
0	0.775
10	0.811
20	0.825
30	0.843
40	0.869
50	0.876
60	0.882
70	0.888
80	0.892
90	0.895
100	0.898
110	0.900
120	0.900
130	0.900
140	0.900
150	0.898
160	0.895
170	0.892
180	0.887
190	0.882
200	0.875
210	0.867
220	0.857
230	0.845
240	0.830
250	0.811
260	0.755
270	0.697
280	System Collapse

As the solar PV capacity increases from 150 MW to 270 MW, the voltage magnitudes begin to decrease. This occurs because utilizing larger solar PV capacities over a long operational period can lead to instability. Furthermore, solar PV primarily injects real power into Bus 18 without providing sufficient reactive power support. Therefore, when the solar PV capacity reaches 280 MW, Bus 18 collapses, indicating its failure and inability to maintain voltage magnitude values. To summarize, the suitable solar PV capacity for Bus 18 at a 30% load increment ranges between 110 MW to 140 MW.

At a 60% load increment, the maximum load capacity at Bus 18 reaches 111.41 MW and 40.14 MVAR. Table 4 presents the voltage magnitude results after integrating various solar PV capacities at these maximum load values.

Table 4 Solar PV integration at Bus 18 under 60% load increment

Solar PV Capacity (MW)	Voltage Magnitude (pu)
0	0.733
10	0.757
20	0.796
30	0.810
40	0.829
50	0.836
60	0.863
70	0.870
80	0.876
90	0.880
100	0.884
110	0.886
120	0.888
130	0.889
140	0.889
150	0.888
160	0.886
170	0.884
180	0.880
190	0.875
200	0.869
210	0.862
220	0.853
230	0.842
240	0.829
250	0.813
260	0.764
270	0.727
280	System Collapse

The suitable solar PV capacity for Bus 18 at a 60% load increment ranges between 130 MW to 140 MW, achieving a maximum voltage magnitude of 0.899 pu. Previously, it was mentioned that the standard voltage stability range is between 0.95 pu to 1.05 pu for a system to be considered stable. However, the current voltage magnitude only reaches 0.889 pu which is still below 0.95 pu. This is due to Bus 18 operating under higher maximum load conditions.

3.5 Solar PV Integration at the Identified Most Stable Bus

Table 5 illustrates the integration of solar PV at Bus 23 with a maximum load of 146.9 MW and 48.91 MVAR at 30% load increments.

Table 5 Solar PV integration at Bus 23 under 30% load increment

Solar PV Capacity (MW)	Voltage Magnitude (pu)
0	0.709
10	0.742
20	0.759
30	0.774
40	0.788
50	0.801
60	0.813
70	0.838
80	0.848
90	0.858
100	0.867
110	0.875
120	0.883
130	0.891
140	0.898
150	0.905
160	0.912
170	0.918
180	0.924
190	0.930
200	0.935
210	0.941
220	0.946
230	0.951
240	0.955
250	0.960
260	0.964
270	0.968
280	0.972
290	0.976
300	0.979

The first observation is that the voltage magnitude continues to rise even with an increase in solar PV capacity up to 300 MW. However, at Bus 18, the maximum solar PV that can be supplied is only 270 MW, and the voltage magnitude drops to around 0.7 pu. This section focuses only on the 30% load increments, as the voltage magnitude values can still increase even with a solar PV capacity up to 300 MW.

3.6 Optimal Placement and Adaptive Solar PV Capacity

Based on the results in Sections 3.4 and 3.5, the optimal placement for solar PV is only at the weakest bus. This is because there is no need for a higher capacity solar PV at the more stable bus. Installing solar PV at the weakest bus is also an effective way to address voltage stability issues. It can be concluded that the most stable bus requires a greater solar PV capacity to be installed. However, a higher capacity solar PV also leads to higher installation costs.

Since solar PV is installed at the weakest bus, the suitable capacity at a 30% load increment ranges from 110 MW to 140 MW, while at a 60% load increment, the range is 130 MW to 140 MW. Therefore, 130 MW is the most suitable solar PV capacity to install as it can effectively support both load increments.

3.7 VCPI Comparison Before and After Solar PV Integration

Figure 4 presents the VCPI values before and after installing solar PV at the weakest bus. The blue bars indicate a lower value after the installation of solar PV, demonstrating its effectiveness in solving voltage stability issues.

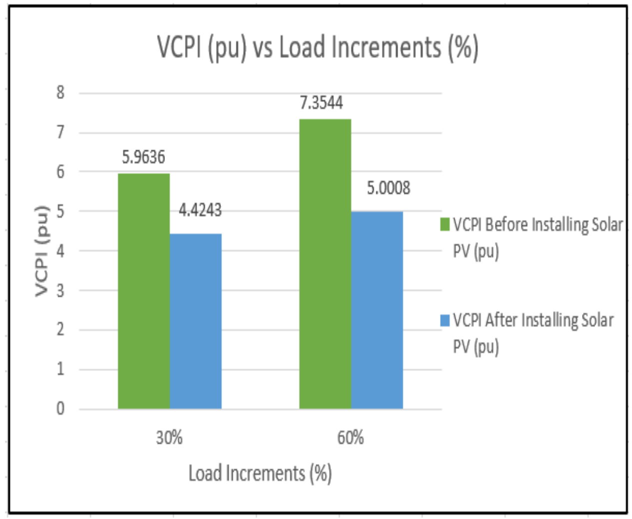

Figure 4 Comparison of VCPI values before and after solar PV installation

As previously mentioned, the VCPI value must be close to zero to be considered stable. However, the current VCPI values are 4.4243 pu and 5.0008 even after installing solar PV. One reason for this is that, at a 30% load increment, the maximum voltage magnitude only reaches 0.9 pu. This value does not reach 1.0 pu, which is considered the ideal voltage in the power system context.

Another reason is the way the VCPI equation is formulated. The equation does not account for power generation from the sending end. For example, when a 130 MW solar PV system is installed at the weakest bus, this additional power is not included in the equation. However, in reality, power generation increases due to the presence of solar PV. Since the equation does not consider this increase, it may result in the VCPI failing to approach zero.

4.0 CONCLUSION

This research focuses on the voltage stability assessment of large-scale photovoltaic systems. The study analyzes voltage stability on the IEEE 57-bus test system and proposes a strategic placement and capacity for installing solar PV at the associated bus. The findings highlight that by implementing the Voltage Collapse Proximity Index (VCPI), the study identifies critical buses prone to instability, specifically Bus 18, while the most stable bus is Bus 23. The results indicate that after installing solar PV on both buses, it is concluded that only the weakest bus requires PV installation. The optimal and strategic placement of solar PV is determined to be at Bus 18 with a capacity of 130 MW. The significance of this research is to sustain and enhance the electric power network, especially in areas experiencing rapid growth and increasing electricity demand. In conclusion, adaptive solar PV integration can optimize voltage stability and withstand higher load conditions without causing stability issues. In future work, the formulation of the VCPI equation can be improved by including power generation from the sending end such as the solar PV capacity into the equation. This will ensure a more accurate assessment of voltage stability and allow the VCPI results to approach zero after solar PV installation.

Acknowledgement

The authors gratefully acknowledge the support and funding from Universiti Tun Hussein Onn Malaysia (UTHM) through Tier 1 Grant Vot (Q878).

Conflicts of Interest

The author(s) declare(s) that there is no conflict of interest regarding the publication of this paper.

References

[1] E. Kocak, E. E. Ulug, and B. Oralhan. 2023. The Impact of Electricity from Renewable and Non-Renewable Sources on Energy Poverty and Greenhouse Gas Emissions (GHGs): Empirical Evidence and Policy Implications. *Energy.* 272: 127125. DOI: 10.1016/j.energy.2023.127125.

[2] Majeed Butt, O., Zulqarnain, M., and Majeed Butt, T. 2021. Recent advancement in smart grid technology: Future prospects in the electrical power network. *Ain Shams Engineering Journal.* 12(1): 687–695. DOI: 10.1016/j.asej.2020.05.004.

[3] Vita, V., Fotis, G., Pavlatos, C., and Mladenov, V. 2023. A New Restoration Strategy in Microgrids after a Blackout with Priority in Critical Loads. *Sustainability.* 15(3): 1974. DOI: 10.3390/su15031974.

[4] Amusan, O. T., Nwulu, N. I., and Gbadamosi, S. L. 2022. Identification of weak buses for optimal load shedding using differential evolution. *Sustainability.* 14(6): 3146. DOI: 10.3390/su14063146.

[5] Liang, X., Chai, H., and Ravishankar, J. 2022. Analytical methods of voltage stability in renewable dominated power systems: A review. *Electricity.* 3(1): 75–107. DOI: 10.3390/electricity3010006.

[6] Calma, E. R. B., and Pacis, M. C. 2021. Artificial neural network-based voltage stability analysis of power transmission networks with distributed generation using phasor measurement unit synthetic data. *2021 IEEE 12th Control and System Graduate Research Colloquium (ICSGRC*). 1–6.

[7] Fasina, T., Adebanji, B., Abe, A., and Ismail, I. 2021. Impact of distributed generation on the Nigerian power network. Indonesian *Journal of Electrical Engineering and Computer Science.* 21(3): 1263–1270. DOI: 10.11591/ijeecs.v21.i3.pp1263-1270.

[8] Nappu, M. B., Arief, A., and Maulidah, A. 2021. Voltage stability analysis of an interconnected power system considering varied output of wind power plants. *Journal of Southwest Jiaotong University.* 56(3): 111–123. DOI: 10.35741/issn.0258-2724.56.3.10.

[9] Mokred, S., and Wang, Y. 2024. Voltage stability assessment and contingency ranking in power systems based on modern stability assessment index. *Results in Engineering.* 23: 102548. DOI: 10.1016/j.rineng.2024.102548.

[10] Chaithra, A., and Modi, S. 2018. Power system vulnerability assessment using voltage collapse proximity index. *2018 2nd IEEE International Conference on Power Electronics, Intelligent Control and Energy Systems (ICPEICES)*. 39–43.

[11] Kushwaha, P. K., and Bhattacharjee, C. 2020. A research on selection of appropriate stability index under adverse system conditions for the assessment of voltage stability of an IEEE 14 bus power system. *European Journal of Electrical Engineering* 22(6): 435–446. DOI: 10.18280/ejee.220605.

[12] Chaithra, A., and Modi, S. 2018. Evaluation of power system stability using voltage proximity index. *2018 International Conference on Recent Innovations in Electrical, Electronics & Communication Engineering (ICRIEECE).* 1537–1540.

[13] Thota, P. K., Somaskandan, G., and Mani, M. 2023. The voltage stability analysis for grid-connected PV system using optimized control tested by IEEE 14 & 30 bus system. *International Journal of Experimental Research and Review* 30: 109–118. DOI: 10.52756/ijerr.2023.v30.012.

[14] Ibrahim, M. H., Ang, S. P., Dani, M. N., Petra, R., and Salam, M. A. 2023. Voltage stability assessment for solar photovoltaic penetration using reactive power–voltage and active power–voltage modal analysis. *Energy Reports* 9: 486–493. DOI: 10.1016/j.egyr.2023.05.124.

[15] Kim, D., Hoang, H. T., and Khanh, N. P. 2022. Simulation research on interaction between wind and solar photovoltaics systems*. ASEAN Engineering Journal* 12(1): 141–148. DOI: 10.11113/aej.v12.17265.

[16] Ansori, A., Arsana, I. M., Siregar, I. H., Adiwibowo, P. H., and Haryuda, S. I. 2023. Techno-economic analysis of triangular rooftop solar PV model/PLN on-grid household scale in Indonesia. *ASEAN Engineering Journal* 13(4): 127–132. DOI: 10.11113/aej.v13.19858.

[17] Ullah, Z., Elkadeem, M. R., Wang, S., and Akber, S. M. A. 2020. Optimal planning of RDS considering PV uncertainty with different load models using artificial intelligence techniques. I*nternational Journal of Web and Grid Services* 16(1): 63. DOI: 10.1504/IJWGS.2020.106126.

[18] Ullah, Z., Elkadeem, M. R., Wang, S., Sharshir, S. W., and Azam, M. 2020. Planning optimization and stochastic analysis of RE-DGs for techno-economic benefit maximization in distribution networks. *Internet of Things.* 11: 100210. DOI: 10.1016/j.iot.2020.100210.

[19] Anand, R., and Balaji, V. 2015. Power flow analysis of Simulink IEEE 57 bus test system model using PSAT. *Indian Journal of Science and Technology.* 8(23). DOI: 10.17485/ijst/2015/v8i23/79266.

[20] Chatterjee, D. 2014. C*omputer Techniques and Models in Power Systems.* 3rd ed. McGraw Hill Education.

[21] Nur and A. Kaygusuz. 2021. Load flow analysis with Newton–Raphson and Gauss–Seidel methods in a hybrid AC/DC system. *IEEE Canadian Journal of Electrical and Computer Engineering.* 44(4): 529–536. DOI: 10.1109/ICJECE.2021.3097447.

[22] Samburi, N., and Nor, A. F. M. 2025. A comparative study of Gauss-Seidel and Newton-Raphson methods in power flow analysis. *Multidisciplinary Applied Research and Innovation*. 6(2): 89–95.

[23] Ashwin, N., Sreedevi, J., Dixit, P., and K S, M. 2019. Voltage stability of power system using PV curve and PMU data. *International Journal of*

Recent Technology and Engineering (IJRTE). 8(3): 7654–7659. DOI: 10.35940/ijrte.C6227.098319.

[24] Yu, L. 2018. Matlab programming environment based on web. 2018 *IEEE 4th Information Technology and Mechatronics Engineering Conference (ITOEC)*. 509–512.

[25] Chandan, A. 2023. IEEE 30 bus Newton Raphson load flow analysis. *MATLAB Central File Exchange.* Retrieved December 16, 2023. https://www.mathworks.com/matlabcentral/fileexchange/58884-ieee-30-bus-newton-raphson-load-flow-analysis.

[26] Anggara, D., Danial, D., and Abidin, Z. 2025. Analysis of the effect of increasing load on voltage profile in electric power distribution system. *Action Research Literate.* 9(9): 2095–2103. DOI: 10.46799/arl.v9i9.3033.

[27] Chaithra, A., and Modi, S. 2018. Evaluation of power system stability using voltage proximity index. *2018 International Conference on Recent Innovations in Electrical, Electronics & Communication Engineering (ICRIEECE).* 1537–1540.